Asymptomatic spread of huanglongbing and implications for disease control

Jo Ann Lee[a,1], Susan E. Halbert[b], William O. Dawson[c], Cecile J. Robertson[c], James E. Keesling[a], and Burton H. Singer[d,1]

[a]Department of Mathematics, University of Florida, Gainesville, FL 32611-8105; [b]Division of Plant Industry, Florida Department of Agriculture and Consumer Services, Gainesville, FL 32608-1201; [c]Department of Plant Pathology, Citrus Research and Education Center, University of Florida, Lake Alfred, FL 33850-2243; and [d]Emerging Pathogens Institute, University of Florida, Gainesville, FL 32610-0009

Contributed by Burton H. Singer, April 29, 2015 (sent for review September 22, 2014; reviewed by Christopher A. Gilligan and Alan Hastings)

Huanglongbing (HLB) is a bacterial infection of citrus trees transmitted by the Asian citrus psyllid *Diaphorina citri*. Mitigation of HLB has focused on spraying of insecticides to reduce the psyllid population and removal of trees when they first show symptoms of the disease. These interventions have been only marginally effective, because symptoms of HLB do not appear on leaves for months to years after initial infection. Limited knowledge about disease spread during the asymptomatic phase is exemplified by the heretofore unknown length of time from initial infection of newly developing cluster of young leaves, called flush, by adult psyllids until the flush become infectious. We present experimental evidence showing that young flush become infectious within 15 d after receiving an inoculum of *Candidatus Liberibacter asiaticus* (bacteria). Using this critical fact, we specify a microsimulation model of asymptomatic disease spread and intensity in a grove of citrus trees. We apply a range of psyllid introduction scenarios to show that entire groves can become infected with up to 12,000 psyllids per tree in less than 1 y, before most of the trees show any symptoms. We also show that intervention strategies that reduce the psyllid population by 75% during the flushing periods can delay infection of a full grove, and thereby reduce the amount of insecticide used throughout a year. This result implies that psyllid surveillance and control, using a variety of recently available technologies, should be used from the initial detection of invasion and throughout the asymptomatic period.

asymptomatic huanglongbing | latent period | transmission model | control strategies

The main symptoms of huanglongbing (HLB) in citrus trees are yellow shoots, leaves with blotchy mottle, and small lopsided fruits. Ultimately, infected branches die back and the tree dies. The putative causal agent of HLB is an alpha-proteobacterium, *Candidatus Liberibacter asiaticus* (*Ca.* Las), that resides within the phloem and is transmitted by the Asian citrus psyllid *Diaphorina citri* Kuwayama. The highest concentrations of *Ca.* Las in infected trees are in the stem and midribs of flush. The flush is a newly developing cluster of very young leaves on the expanding end of a terminal shoot. The bacterium multiplies in both the psyllids and the trees, but the psyllids are essential for the spread of the disease.

The dominant control measure currently in use is the combination of insecticidal spraying to limit the psyllid populations and removal of infected trees, an inoculum source, when they are symptomatic. This strategy has had only marginal effect because symptoms appear anywhere from months to years after an initial infection, long after the trees have been active in the transmission process (1). Presymptomatic trees can serve as a source of inoculum for psyllids, but the length of time from initial infection of a tree until it is infective as a source of inoculum is known from experimental measurements only to within coarse bounds (within 60 d) (1). An alternative statistical approach to infer latent and incubation periods from successive snapshots of symptom spread in groves has recently been published (2) (*SI Appendix*, section S.2). This particular knowledge gap has limited the development of defensible transmission models that can account for the rapid proliferation of infection in a grove of citrus trees and also provide useful guidance about new control strategies. There also has been a lack of adequate methodology for low-cost sampling and assaying of asymptomatic trees to ascertain whether or not they are infected, and thereby in need of application of control measures to limit spread.

Understanding the rapid spread of psyllids, up to 12,000 psyllids on a single tree accumulating during a 60-d flush period, and, correlatively, the infection of varying levels of intensity in the flush and psyllid populations throughout groves is facilitated by the use of spatially explicit agent-based transmission models within which the geometry of psyllid invasion patterns, psyllid demography, pathways of infection between psyllids and young flush, and intertree migration are taken into account. Our primary concern is transmission from initial invasion of a grove and the spread of infection and its intensity while trees are asymptomatic. To date, HLB transmission models have been deterministic and stochastic compartmental models, where systems of ordinary differential equations represent the dynamics (2–5). The geometry of groves and the foci of psyllid entry generally are not taken into consideration in these models, despite the fact that they clearly influence the initial spread of HLB and the distribution of symptomatic trees on the longer time scale of 1–2.5 y or, as recently documented, 6 y (6). Spatially explicit modeling, however, is incorporated in a recent study of HLB epidemic outbreaks (2). Although our specific focus and the comments above pertain to HLB, it is important to note that there is a considerable literature using spatially explicit models of transmission of plant pathogens incorporating both compartment models (7) (*SI Appendix*, refs. 10–14) and agent-based models (8, 9).

Significance

Huanglongbing (HLB) is a vector-transmitted bacterial infection of citrus trees that poses a major threat to the citrus industry in Florida, Texas, and California. Current control strategies that focus on the vector, the Asian citrus psyllid *Diaphorina citri*, are usually initiated when the trees become symptomatic, anywhere from 10 mo to several years after initial infection. We show, experimentally, that newly infected young leaves can become infectious within 10–15 d after receiving an inoculum of bacteria from an adult psyllid. We then show by microsimulation of the asymptomatic spread of HLB through a grove under different invasion scenarios and control strategies that reduction of up to 75% of adult psyllids and nymphs can enhance citrus production.

Author contributions: J.A.L., S.E.H., W.O.D., C.J.R., J.E.K., and B.H.S. designed research; J.A.L., S.E.H., W.O.D., and C.J.R. performed research; J.A.L., J.E.K., and B.H.S. analyzed data; and J.A.L. and B.H.S. wrote the paper.

Reviewers: C.A.G., University of Cambridge; and A.H., University of California, Davis.

The authors declare no conflict of interest.

Freely available online through the PNAS open access option.

[1]To whom correspondence may be addressed. Email: joann5@ufl.edu or bhsinger@epi.ufl.edu.

This article contains supporting information online at www.pnas.org/lookup/suppl/doi:10.1073/pnas.1508253112/-/DCSupplemental.

Two forms of delays are important for the modeling of the spread of HLB across a grove. These delays are as follows: (*i*) the time from initial infection of young flush on a tree until the onset of disease symptoms and (*ii*) the time from initial infection of young flush by adult psyllids until the flush become infectious. An experimental study shows a minimum time to symptoms of ~200 d and a latent period bounded above by 60 d (1).

The purposes of this paper are as follows: (*i*) to present new experimental evidence on the elapsed time from initial infection of young flush until the flush become infectious to previously uninfected adult psyllids and to nymphs; (*ii*) to describe an agent-based transmission model that can mechanistically produce the spatial patterns of rapid proliferation of *Ca.* Las infection and its intensity in response to a variety of spatially explicit psyllid invasion scenarios in groves of previously uninfected citrus trees, emphasizing the asymptomatic period; and (*iii*) to demonstrate, via modeling, the potential impact of surveillance and intervention strategies applied while trees are asymptomatic and focused on reduction of adult psyllids, as well as nymph stages, in the psyllid life cycle.

Time to Infectiousness of Citrus Flush Following an Initial Infection by Psyllids

Experimental Infections. Psyllids were obtained from an existing psyllid colony that originated in Florida citrus groves. The colony currently is maintained in growth rooms on source plants containing *Ca.* Las originally inoculated in 2007 from symptomatic field trees located in Hendry County, Florida (10). The original objective of these 16 small experiments was simply to ascertain whether or not a new generation of infected adult psyllids would be produced (more details are provided in *SI Appendix*). Generally, six to 10 previously uninfected plants were used for each experiment, with 50 or 100 adult psyllids collected randomly from HLB-infected plants within a plant containment room and added to cages. After 15 d, all adult psyllids from the input population were removed and a random sample of 24 of these adult psyllids was stored in a freezer for subsequent DNA extraction. After 30 d, a random sample of 24 of psyllid progeny (output) that emerged from eggs deposited by the input psyllids was also removed and stored in a freezer. DNA was extracted from individual psyllids using a Qiagen DNeasy Blood & Tissue Kit according to the manufacturer's recommendations. Plant samples (300 mg) were extracted in 3 mL of extraction buffer [100 mM Tris·HCl (pH 8.0), 50 mM EDTA, 500 mM NaCl, and 10 mM DTT] as described previously (10). Conventional PCR and quantitative PCR (qPCR) analyses were conducted as also described previously (11).

Results. Table 1 shows the percentages of *Ca.* Las-positive psyllid progeny infected through exposure to *Citrus macrophylla* that were infected by a prior generation of adult psyllids. The results in Table 1 show that psyllid progeny acquired *Ca.* Las from plants that were not infected with HLB 30 d earlier. This time frame was sufficient for the plants to become efficient donor hosts. It is known that psyllids have higher titers of *Ca.* Las when the bacterium is acquired by nymphs (12). Thus, the assayed adult progeny psyllids would have had to acquire the bacterium at a time earlier than 30 d. Adults emerge after 15 d, and 22 d was the earliest time of detection of infectiousness in flush. Psyllids did not lay eggs on all plants in each cage. Usually about one-third to one-half of the plants were infested with nymphs. The plant samples that were analyzed by PCR for *Ca.* Las sequences were taken from locations where nymphs developed. Plant samples that were taken at 10–15 d already tested positive for *Ca.* Las. The results confirm that the areas of the plants where psyllid progeny developed could become infected with *Ca.* Las within this short time period, and thereby serve as a source of inoculum for the developing nymphs.

The present experiment was conducted using *C. macrophylla*, as opposed to *Citrus sinensis*, which is grown in most of the commercial groves, because psyllids seem to like this host slightly better and the plants are easier to maintain and have more flush in the greenhouse than *C. sinensis*. The essential difference between these species is that with time, usually 6–12 mo after infection, disease symptoms are more severe in *C. sinensis* under greenhouse conditions (13). However, the time course of accumulation of *Ca.* Las in both of these species is similar (10, 11).

Transmission Model

We introduce a spatially explicit simulation model that is analogous to an earlier model of transmission of arthropod-vectored plant viruses (14) (more on choice of model is provided in *SI Appendix*). Here, however, we focus on transmission of the bacteria *Ca.* Las between the psyllid vector, *D. citri*, and young flush shoots on the trees. Treating a tree as a flush patch is a key feature of the model, an emphasis first put forth by Chiyaka et al. (3). To relate the local transmission mechanism at flush shoots to the spread through a grove, we identify patches of flush and groups of psyllids with points on a 2D grid, representing a grove of citrus trees. We are not only concerned with the infection status of flush patches and psyllids on them but with the intensity of infection in psyllid and flush populations at each location. We score intensity by the proportion of flush that are infected at each patch and by the proportion of psyllids at that patch that are infected. We make essential use of the very short latency period supported by the experiment described in the previous section. This short latency period is consequential for the rapid infection of nymphs and previously uninfected adult psyllids on the newly infected flush. It is important to note that the short latency period experimentally determined here is consistent with the cyclic exponential and Weibull models for duration of latency period used by Parry et al. (2). The long asymptomatic period of the tree is accompanied by the rapid spread of infection among psyllids and new flush, thereby leading to large percentages, even 100%, of trees infected in a grove before any symptoms become manifest. This rapid asymptomatic spread places a premium on intensive psyllid

Table 1. Infection of psyllid progeny by *Ca.* Las acquired from *C. macrophylla* infected by the prior generation of adult psyllids

Experiment no.	No. of input psyllids	No. of plants/no. of with nymphs	% *Ca.* Las^{+} input psyllids	% *Ca.* Las^{+} psyllid progeny	No. of plants positive*/total†
1	50	6/2	25‡	38 @ 30 d	2/2 @ 30 d
2	50	6/2	21§ (33‡)	0 @ 30 d	0/2 @ 30 d
3	50	6/2	33‡	33 @ 30 d	1/2 @ 30 d
4	50	6/6	24‡	5 @ 30 d	2/4 @ 10 d 3/4 @ 15 d
5	50	6/2	55§	5 @ 30 d	2/2 @ 33 d
6	50	6/2	69§	13 @ 31 d	1/2 @ 33 d
7	50	6/1	29§	8 @ 31 d	1/1 @ 31 d
8	50	6/1	38§	13 @ 31 d	1/1 @ 31 d
9	50	4/2	54§	22 @ 31 d	1/2 @ 30 d
10	50	4/2	100§	54 @ 30 d	2/2 @ 30 d
11	100	10/6	51§	16 @ 30 d	4/6 @ 32 d
12	50	6/nd	5§ (21‡)	12 @ 30 d	nd
13	50	6/nd	17§ (21‡)	0 @ 22 d	nd
14	50	6/nd	8§ (21‡)	17 @ 22 d	nd
15¶	nd	6/2	nd	83 @ 30 d	2/2 @ 38 d
16¶	nd	3/3	nd	29 @ 30d	3/3 @ 58 d

nd, not determined.

*qPCR and PCR detection of *Ca.* Las in infected areas of plants that harbored eggs and nymphs before 30 d.

†Total number of plants that harbored eggs and nymphs before 30 d.

‡Percentage of *Ca.* Las-positive psyllids in the population on HLB-infected plants from which the input psyllids were removed.

§Percentage of *Ca.* Las-positive input psyllids withdrawn from the cages at 15 d.

¶Experiments used psyllid progeny from earlier experiments.

control and the necessity of surveillance of psyllid populations in asymptomatic groves.

Microsimulation Modeling of Transmission. We focus on movement of *Ca.* Las between psyllids and patches of flush as the units of analysis, ignoring within-tree consequences of infection. This decision prioritizes young flush as the sites of initial infection on trees and their role as infectious agents. *Ca.* Las can move from tree to tree via migration of infected adult psyllids. We introduce the day as the time step for transmission activities. For the vectors, we keep track of age and infection status (infected or not) of individual adult psyllids, eggs, and the five instar stages, which we label nymphs. For young flush, we keep track of their age since emergence, their occupancy by eggs and nymphs, and their infection status (uninfected, infected but not infectious, and infectious). In the model, a grove of trees (or a set of flush patches) is an 11×25 lattice with integer coordinates $\mathbf{c} = (c_1, c_2)$. Although flush patches are evenly spaced in this formal specification, the close spacing of trees within a row and the wide between-row spacing in a real grove (*SI Appendix*, Fig. S1) are taken into account by our assuming much higher probabilities of within-row relative to between-row migration of adult psyllids. We assume that there are three flushing seasons: spring (60 d at 25 °C), summer (30 d at 28 °C), and fall (15 d at 25 °C).

We summarize the vector and flush development processes and the accompanying transmission dynamics in our model by describing the activities that take place on a typical day during a flush season. A full algorithmic description of the system dynamics is presented in *SI Appendix*. There are six steps that occur on a flush patch located at a generic site with coordinates $\mathbf{c} = (c_1, c_2)$. In their order of execution, these steps are (*i*) emergence of new flush shoots, (*ii*) migration of adult psyllids to new flush patches, (*iii*) psyllid aging and mortality, (*iv*) egg laying and egg survival, (*v*) *Ca.* Las transmission from infectious flush to nymphs, and (*vi*) *Ca.* Las transmission from adult psyllids to flush. Parameters specified by a numerical value followed by a second value in parentheses are temperature-dependent and correspond to 25 °C (and 28 °C). Parameters used in the simulation model are given in Table 2:

i) Emergence: Each day during a flushing period, 20 new flush, unoccupied by psyllids, emerge at **c**. They join cohorts of 20 flush each that emerged on previous days in the flushing period. Flush from previous days may be occupied by eggs, nymphs, and adults, each identified by an infection status. Flush from prior days also have an infection status (uninfected, infected but not infectious, or infectious). Young flush are regarded as such for 13 (16 at 28 °C) d, after which they are transferred to the category "old," along with their resident psyllid populations.

ii) Migration: Adult psyllids at **c** each have a probability of 0.4 of migrating on the given day. Conditional on being selected to migrate, a psyllid at **c** in the interior of the grove can move to $(c_1 \pm 1, c_2)$ with a probability of 0.025 for each option or to $(c_1, c_2 \pm 1)$ with a probability of 0.475 for each option. Psyllids from each of the above four destinations can, correspondingly, migrate to **c** according to the same rules operating at their points of origin. In-migrants distribute themselves among flush by selecting a shoot with probability $[\text{number of flush shoots}]^{-1}$. At the end of the site transfers, we have lists of infected and uninfected male and female adult psyllids at each flush shoot at locality **c.** Psyllids at boundary locations in the grove can only migrate to three possible nearest neighbors, unless they are at a corner, in which case there are just two options (full details are provided in *SI Appendix*).

iii) Psyllid aging and mortality: Each nymph has probability s_n of surviving to the next day. Nymphs that survive for 13 (11 at 28 °C) consecutive days after initiating nymph status emerge as adult psyllids. Emerging adults on the given day have probability s_a of surviving to the next day, at which time they can take part in *Ca.* Las transmission to flush if they are infected. Adult psyllids already present in the flush patch are also selected with probability s_a for survival and participation in the transmission process (step *vi* below) on the given day. The survivors are labeled according to gender, infection status, and flush shoot identifier. Nymphs are labeled by flush shoot identifier and infection status.

iv) Egg laying and egg survival: Each young flush shoot can accommodate up to 40 eggs per day. Each female psyllid lays 10 eggs each day. On a given day, let $|A|$ be the number of available egg sites on a given flush shoot. The number of newly laid eggs by the $|F|$ female psyllids on the given shoot is $\min[10 \times |F|, |A|]$. Each of the eggs, new + [number surviving from the previous day], is a candidate for survival with probability s_e. After day 13 (16 at 28 °C) in the flushing period, there are 260 (320 at 28 °C) young flush shoots in a patch. This number remains fixed, because on each consecutive day, 20 new flush shoots emerge and 20 shoots are transferred to the old category. The total daily egg capacity of a patch during this time is 40×260 (320 at 28 °C) = 10,400 (12,800 at 28 °C) locations.

v) Transmission from flush to nymphs: Infectious flush shoots have a probability of 0.083 per day of transferring *Ca.* Las to nymphs that are 6 d or more into this stage of development. One can consider this probability to include transovarial transmission, which has been shown to be at around 2–6% (22). Once a nymph becomes infected, it remains so and emerges as an infected adult psyllid 18 (15 at 28 °C) d following the laying of the egg. Emerging infected adults are assumed to be immediately infectious (21).

vi) Transmission from adult psyllids to flush: Adult psyllids feed once per day. They each select a flush shoot at random from those flush shoots present on the given day. An infected psyllid then transmits *Ca.* Las to the selected shoot with a probability of 0.3. If the flush shoot was previously infected, it simply remains infected. A previously uninfected shoot acquires infection. We assume that it becomes infectious 15 d later.

Table 2. Parameters used in simulation model

Parameter description	Value	Units	Source
Maximum flush age	30	d	(15)
Flush shoots emerging	20	d^{-1}	Calculated*
Egg-to-adult transition	17 (14)†	d	(16, 17)
Duration of young flush	13 (16)†	d	Calculated
Proportion of migrating adults	0.4	d^{-1}	Assessed
Within-row probability	0.95		Assessed
Between-row probability	0.05		Assessed
Egg duration	4 (3)†	d	(17)
Nymph duration	13 (11)†	d	(17)
Daily flush shoot capacity	40	Eggs	Calculated*
Eggs laid per female adult	10	Eggs	(18)
Transmission from flush to nymphs	0.083	d^{-1}	Assessed‡
Transmission from adult to flush	0.3	d^{-1}	Assessed
Latent period	10–21	d	Assessed‡
Egg/nymph survival probability	0.8614 (0.8343)†	d^{-1}	(19)
Adult survival probability	0.9847 (0.9659)†	d^{-1}	(17, 20)*
Nymph infection age	9 (8)†	d	(17, 21)

d, days.
*Calculation found in section demographic parameter values.
†Values represent simulation parameters for 25 °C (28 °C).
‡Values assessed from experiments in Table 1 (details are provided in *SI Appendix*).

The above steps are repeated on each day during a flushing season, with appropriate modifications for the first 12 (15 at 28 °C) d, when the population of young flush is growing by 20 shoots per day, and there is no transfer of flush to the old category (algorithmic details are provided in *SI Appendix*).

Initial Conditions. For an initially uninfected grove, we start simulation of the transmission process by placing 200 psyllids on either a few trees in a corner of the grove or on selected trees along an edge of the grove. The latter specification is consistent with considerable evidence about how new waves of psyllids arrive at a grove, frequently driven in by the wind. Hall and Hentz (23) used sticky traps to capture psyllid movement in and out of groves during arbitrary times in the year, with a peak time being in the spring. Boina et al. (24) documented movement in both directions between managed and unmanaged groves. We assume that ∼30% of the initial psyllid population is infected. Newly arrived female psyllids initiate egg laying, and both male and female psyllids feed on flush. These initial conditions initiate the dynamics described above.

Demographic Parameter Values. Daily survival probabilities of the egg and nymphal stages of psyllids are based on field experiments. The percentage of first-instar nymphs that survive to adulthood (19) is 7.91%. There is no field estimate for the survival of eggs, so we assume their survival is the same as the nymph stages to account for the high survival rate found in laboratories and the predation that occurs in the field. The daily survival rates for eggs and nymphs at 25 °C is $(0.0791)^{1/17} = 0.8614$, where 17 is the number of days after which the transition from egg to adult (16) occurs. The adult psyllid daily survival probability was estimated using a $t_{1/2}$ of 45 d via $(1/2)^{1/45} = 0.9847$ (17, 20). In addition, in field observations, we find, on average, 100 eggs per flush shoot. It is assumed that eggs become nymphs in 3 d. This assumption implies that the number of eggs laid on a flush shoot per day, N_e, satisfies the equation, $N_e[1 + 0.8614 + 0.8614^2] = 100$. Solving this equation yields $N_e \approx 40$, which corresponds to four female psyllids laying up to 10 eggs each on a flush shoot on a given day. To obtain a plausible value for the number of new flush per day during a flush period, we assume that a total of 24,000 psyllids can be in a flush patch at the end of a 60-d flush period. Field evidence indicates that 30,000–40,000 psyllids (25) can be on a single tree (equals a flush patch in the simulations). Allowing for a maximum of 20 psyllids per flush yields 1,200 flush accumulating over 60 d. Thus, the number of new flush per day, N_f, should be $N_f = 20$.

Results

Six sets of invasion conditions are introduced to convey the variation in rate of spread of infection consequential to them. These sets are as follows: (*i*) 200 psyllids, 30% of which are infected, are placed on four trees in the southwest corner of the grove; (*ii*) condition *i* AND 35% of randomly selected trees are occupied by 200 uninfected psyllids; (*iii*) 200 psyllids, 30% of which are infected, are placed on six trees on the southern edge of the grove and on 11 trees on the eastern edge of the grove; (*iv*) condition *iii* AND 35% of randomly selected trees are occupied by 200 psyllids, none of which are infected; (*v*) 10 trees distributed around the center of the grove are occupied by 200 psyllids, 30% of which are infected; and (*vi*) condition *v* AND 35% of randomly selected trees from the remaining 265 sites are occupied by 200 psyllids, none of which are infected. It is assumed that the time from initial infection of a young flush until it becomes infectious is 15 d.

Table 3. Elapsed time (days) from initial invasion until 100% of the trees are infected in the absence of control measures

Invasion condition	Mean time until 100% of trees infected
(*i*) Corner	781 ± 18*
(*ii*) Corner + 35%	450 ± 41*
(*iii*) Edge	424 ± 14*
(*iv*) Edge + 35%	234 ± 57*
(*v*) Middle	400 ± 8*
(*vi*) Middle + 35%	169 ± 11*

*95% confidence interval based on 50 simulation runs.

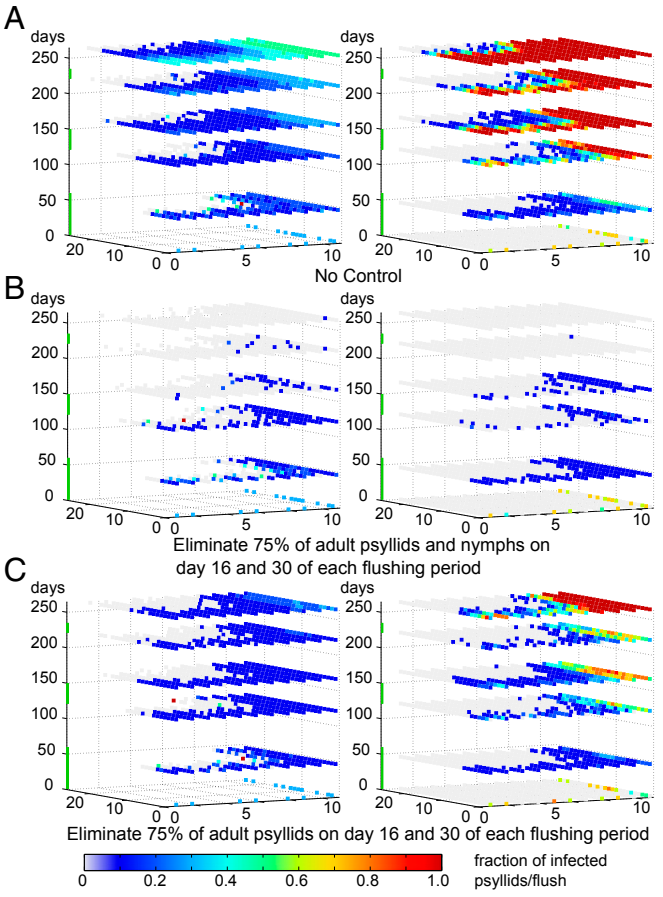

Fig. 1. All panels are for invasion scenario *iii*. No control (*A*), elimination of 75% of adult psyllids and nymphs on days 16 and 30 of each flushing period (*B*), and elimination of 75% of adult psyllids on days 16 and 30 of each flushing period (*C*). Within each panel, the fraction of psyllids infected (*Left*) and the fraction of flush infected (*Right*) are shown. The green segments on the vertical axis (i.e., days since initial invasion of the grove) correspond to flushing periods. Migration of psyllids between trees accounts for the spread through the entire grove. Coordinates in the *x*–*y* plane correspond to locations of trees. In the simulation, we are not assuming trees are evenly spaced (*Microsimulation Modeling of Transmission*).

The central point of the results in Table 3 is that not only the number of trees containing infected psyllids at the start of an invasion but the number of trees initially occupied by uninfected psyllids influences the time to infection of a full grove. Invasion scenarios *i*–*iv* are four of a myriad of possible initial conditions where a given grove is invaded by psyllids from an adjacent grove in a large multigrove system (6). Scenarios *v* and *vi* correspond to two of many possible initial distributions of psyllids that may be blown into a grove by the wind (26). The variation in time until 100% of the trees are infected as shown in Table 1 is undoubtedly an underestimation relative to field conditions in the absence of controls, because multiple psyllid invasions over time are an important feature of the introduction of HLB to a grove. We are entirely lacking empirical investigations of invasion processes in working citrus groves, to say nothing of controlled introductions over time in experimental groves. The important

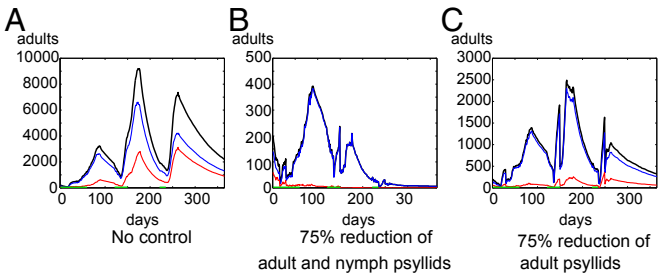

Fig. 2. All panels are for adult psyllid counts on a single tree located at (11,11) under invasion scenario *iii*. For all panels, black lines represent the total adult psyllids, blue lines represent healthy adult psyllids, and red lines represent infected adult psyllids. No control (*A*), elimination of 75% of adult psyllids and nymphs on days 16 and 30 of each flushing period (*B*), and elimination of 75% of adult psyllids on days 16 and 30 of each flushing period (*C*) are shown. The green segments on the horizontal axis (i.e., days since initial invasion of the grove) correspond to flushing periods.

analyses of variable spread rates in replicated invasions described by Melbourne and Hastings (27) are relevant to our problem, and suggest a pressing need for experimental studies of psyllid invasions and attempts to monitor such invasions in natural settings. A more extensive discussion of variable spread rates consequential to psyllid invasions is given in *SI Appendix*.

Fig. 1 shows the advance of infection and the variation of intensities through the grove under scenario *iii*, where infection is introduced along the southern and eastern edges of the grove. We show the results of a strategy where either reduction in adult psyllids or reduction in both adults and nymphs occurs on days 16 and 30 of each flushing period. Here, it is important to emphasize that elimination of adult psyllids without harming nymphs is hypothetical, not corresponding to the use of a known pesticide. There are, however, pesticides that act on nymphs only, as well as pesticides that act on the combination of adults and nymphs. Here, it is assumed that 75% of both adult psyllids and nymphs are eliminated at each attack in Fig. 1*B*, whereas only 75% of adult psyllids are eliminated at each attack in Fig. 1*C*. The sharp contrast between Fig. 1*B* and Fig. 1*C* shows the major role of transmission from infected flush to nymphs, and to emerging adults from them. Failure to control this transmission link has serious consequences for the spread of infection. Overall, there is considerable reduction in the fraction of infected psyllids relative to the intense infection picture (Fig. 1*A*) in the absence of control measures.

The number of psyllids on an individual tree varies over time as indicated in Fig. 2. Peak numbers of psyllids are present after each flushing season begins and after the first emergence of new adult psyllids. Under scenario *iii*, the psyllid count on an individual tree reaches 9,000 during the summer flushing season.

Expanding the discussion, Table 4 contains a coarse-level summary of the impact of four intervention scenarios on the abundance of psyllids and the infection status of populations of them on trees in the simulated 11 × 25 lattice grove. The interventions are (*a*) a 75% reduction in adult psyllids on days 16 and 30 of each flush period, (*b*) a 75% reduction in adult psyllids on days 2 and 30 after the start of each flush period, (*c*) intervention *a* AND a 75% reduction in nymphs on days 16 and 30 of each flush period, and (*d*) intervention *b* AND a 75% reduction in nymphs on days 2 and 30 after the start of each flush period. Statistics are presented for days 151 and 241 in a 1-y cycle. The top figure in each cell is the percentage of trees that are occupied by psyllids. The bottom figure is the number of trees (of a total of 275) in the grove with more than 10% of the occupying psyllids infected.

The important qualitative features of Table 4 are as follows: (*i*) a 75% reduction in adult psyllids alone has the greatest impact when spraying is carried out on days 2 and 30 of each flush period; (*ii*) the most dramatic impact on the reduction of the number of trees occupied by psyllids and a high infection rate among psyllids on a given tree is attained when both adult psyllid and nymph reduction are carried out without damaging the young flush; and (*iii*) without effective control measures, occupancy of many trees by uninfected psyllids at the start of an invasion promotes the spread of infection throughout the grove. A more fine-grained representation of each invasion × intervention scenario, analogous to Figs. 1 and 2, is shown in *SI Appendix*.

Discussion

We have shown experimentally that the latency period from new infection by infected adult psyllids to infectiousness in young flush is less than 15 d. In subsequent experiments, most of the plants that were colonized by psyllids developed HLB symptoms, but those plants that did not have nymphs usually failed to develop disease. These intriguing observations have not been quantified and deserve further study. Using the latency period information in a model where feeding by infected adults on young flush subsequently infects nymphs already on the flush, we showed that entire groves can become infected in a few months. The resulting infected trees can all be asymptomatic, and can become home to on the order of 12,000 psyllids, a large fraction of which are infected, during a single flush period. Because trees do not tend to show symptoms for anywhere from 1–2.5 y, and possibly longer, after initially becoming infected, emphasis must be placed on ongoing surveillance and control of psyllids. The invasion scenarios we consider have the common feature that there is a single invasion occurring on a given day, and all transmission of infection and growth of the psyllid population is consequential to these initial conditions. The psyllid counts on the order of 20,000–30,000 observed on single trees in field settings are a consequence of more intensive invasions that take place over time. For example, the edge invasion scenario followed a few weeks later by a middle-field invasion of psyllids would increase the rate of spread of infection and considerably increase the psyllid count for individual trees.

Our simulations indicate that 75% of reductions in the psyllid population as a result of control strategies carried out during all flush periods in a year can delay the appearance of symptomatic trees by at least 240 d, and by 1 y or more in many instances, beyond what would ensue without such control. If it is feasible to attain a 90% psyllid population reduction compared with the population without psyllid control, groves could be producing

Table 4. Proportion of grove occupied by psyllids (top value) and number of trees out of 275 with more than 10% of the occupying psyllids infected (bottom value) on days 151 and 241 under different invasion *i–vi* and intervention *a–d* conditions

	75% reduction of adult psyllids				75% reduction of adult and nymph psyllids			
	(*a*) Days 16 and 30*		(*b*) Days 2 and 30*		(*c*) Days 16 and 30*		(*d*) Days 2 and 30*	
Invasion condition	Day 151	Day 241	Day 151	Day 241	Day 151	Day 241	Day 151	Day 241
(*i*) Corner	0.324	0.407	0.251	0.287	0.207	0.233	0.218	0.215
	9	16	0	0	0	1	0	0
(*ii*) Corner + 35%	1.00	1.00	1.00	1.00	1.00	1.00	1.00	1.00
	8	34	0	0	0	0	0	0
(*iii*) Edge	0.829	0.902	0.720	0.782	0.724	0.716	0.695	0.716
	6	48	1	0	2	1	0	0
(*iv*) Edge + 35%	1.00	1.00	1.00	1.00	1.00	1.00	1.00	1.00
	63	158	0	0	0	0	0	0
(*v*) Middle	0.844	0.938	0.702	0.793	0.702	0.622	0.640	0.618
	8	29	0	0	0	1	1	0
(*vi*) Middle + 35%	1.00	1.00	1.00	1.00	1.00	1.00	1.00	1.00
	35	111	0	0	0	0	0	0

*Days after the start of each flush period.

fruit free of HLB for 2+ y beyond the time of symptom onset in uncontrolled groves. Such reductions from spraying adult psyllids have been demonstrated in Brazil, for example (28).

The question of how to reach 90% reductions in psyllid populations relative to uncontrolled conditions in a multigrove setting is starting to get serious consideration from grower cooperatives (www.crec.ifas.ufl.edu/extension/chmas/chma_overview.shtml). A critical first step is synchronization of insecticide spraying schedules on a regional basis to reduce movement of psyllids drastically from one grove to the next, as well as to reduce their prevalence within groves. In addition, the use of aluminized mulch (29) to protect newly planted trees for the roughly 2 y it takes before a canopy prevents effective utilization of this methodology has the potential to delay the introduction of psyllids to a grove during this period of early development. Other psyllid control tools are under development and suggest that the stringent targets we have indicated for delaying the onset of symptoms should be within reach.

Psyllid flush transmission is the dominant mode of dispersal of *Ca.* Las in a grove, as demonstrated by the documented large numbers of psyllids that occupy trees in infected groves, as well as the multiple routes of rapid propagation of this bacterium between psyllids and flush. Better surveillance tools are needed to help quantify the progression of new infection in previously uninfected groves. A start on incidence estimation for an epidemic when it is first discovered and the design of early detection monitoring have been put forth recently (30). However, as the intricate asymptomatic transmission illustrated herein indicates, much more needs to be done in this direction.

Materials and Methods

In the experimental study, two plant growth rooms (15 × 19 feet) were prepared with a 14-h photoperiod of photosynthetically active electromagnet radiation (Em) of ∼200 $\mu Em^{-2} \cdot s^{-1}$ using Sylvania T5 fluorescent lamps maintained at ∼26 °C. In addition to *C. macrophylla*, *Carrizo citrange* (× *Citroncirus weberri*) plants were studied at ∼6–12 mo of age and were grown from seed. Further, *Murraya exotica* L. ("orange jasmine") and *Bergera koenigii* L. plants were obtained externally and also included in the study. Results for the latter three plants are shown in *SI Appendix*. We include them because they are part of the HLB transmission system on a regional basis, particularly for initial introductions of infected psyllids to citrus groves. However, it is the within-grove transmission of HLB among asymptomatic trees that is the focus of our modeling exercise, rather than the vastly larger spatial scales involved in intracounty spread. All plants were pesticide-free at the time of experiments. Plants were caged in 24 × 24 × 36-foot collapsible observation and rearing cages and were continuously maintained within the controlled environment growth rooms.

qPCR reactions were carried out using an ABI 7500 (Applied Biosystems) real-time PCR instrument per the manufacturer's instructions using HLBaspr primer/probe sets plus a plant COX-based primer probe set as indicated by Li et al. (31). In the analysis of noninfected plants or psyllids, qPCR often results in a cycle threshold (Ct) value in the 30s. Ct values under 30 were considered confidently positive, but higher numbers were considered ambiguous. We reran all ambiguous samples by conventional PCR and called samples positive that resulted in a distinct band in the correct position (11).

ACKNOWLEDGMENTS. We thank Ariena van Bruggen for helpful comments and criticism on a prior draft. J.A.L. was partially supported by Emerging Pathogens Institute and the Citrus Research and Development Foundation (CRDF) Contract 00094417. W.O.D. was funded by CRDF Contract 00085411 and an endowment from the J. R. and Addie Graves family. This paper is Entomology Contribution No. 1256, Florida Department of Agriculture and Consumer Services, Division of Plant Industry, Bureau of Entomology, Nematology, and Plant Pathology.

1. Coletta-Filho HD, Daugherty MP, Ferreira C, Lopes JRS (2014) Temporal progression of 'Candidatus Liberibacter asiaticus' infection in citrus and acquisition efficiency by Diaphorina citri. *Phytopathology* 104(4):416–421.
2. Parry M, et al. (2014) Bayesian inference for an emerging arboreal epidemic in the presence of control. *Proc Natl Acad Sci USA* 111(17):6258–6262.
3. Chiyaka C, Singer BH, Halbert SE, Morris JG, Jr, van Bruggen AHC (2012) Modeling huanglongbing transmission within a citrus tree. *Proc Natl Acad Sci USA* 109(30):12213–12218.
4. Vilamiu RGA, Ternes S, Braga GA, Laranjeira FF (2012) A model for Huanglongbing spread between citrus plants including delay times and human intervention. *AIP Conf Proc* 1479(1):2315–2319.
5. Jacobsen K, Stupiansky J, Pilyugin SS (2013) Mathematical modeling of citrus groves infected by huanglongbing. *Math Biosci Eng* 10(3):705–728.
6. Shen W, et al. (2013) Occurrence and in-grove distribution of citrus huanglongbing in North Central Florida. *J Plant Pathol* 95(2):361–371.
7. Leclerc M, Doré T, Gilligan CA, Lucas P, Filipe JAN (2014) Estimating the delay between host infection and disease (incubation period) and assessing its significance to the epidemiology of plant diseases. *PLoS ONE* 9(1):e86568.
8. Atallah SS, Gómez MI, Conrad JM, Nyrop JP (2015) A plant-level, spatial, bioeconomic model of plant disease diffusion and control: Grapevine leafroll disease. *J Agr Econ* 97(1):199–218.
9. Holt J, Chacellor TCB (1996) Simulation modeling of the spread of rice tungro virus disease: The potential for management by roguing. *J Appl Ecol* 33(5):927–936.
10. Folimonova SY, Robertson CJ, Garnsey SM, Gowda S, Dawson WO (2009) Examination of the responses of different genotypes of citrus to huanglongbing (citrus greening) under different conditions. *Phytopathology* 99(12):1346–1354.
11. Tatineni S, et al. (2008) In planta distribution of 'Candidatus Liberibacter asiaticus' as revealed by polymerase chain reaction (PCR) and real-time PCR. *Phytopathology* 98(5): 592–599.
12. Hung TH, Hung SC, Chen CN, Hsu MH, Su HJ (2004) Detection by PCR of Candidatus Liberibacter asiaticus, the bacterium causing citrus huanglongbing in vector psyllids: Application to the study of vector-pathogen relationships. *Plant Pathol* 53(1): 96–102.
13. Shokrollah H, Abdullah TL, Sijam K, Abdullah SNA, Abdullah NAP (2009) Differential reaction of citrus species in Malaysia to Huanglongbing (HLB) disease using grafting method. *Am J Agric Biol Sci* 4(1):32–38.
14. Ferriss RS, Berger PH (1993) A stochastic simulation model of epidemics of arthropod-vectored plant viruses. *Phytopathology* 83(12):1269–1278.
15. Hall DG, Albrigo LG (2007) Estimating the relative abundance of flush shoots in citrus with implications on monitoring insects associated with flush. *HortScience* 42(2):364–368.
16. Tsai JH, Liu YH (2000) Biology of Diaphorina citri (Homoptera: Psyllidae) on four host plants. *J Econ Entomol* 93(6):1721–1725.
17. Liu YH, Tsai JH (2000) Effects of temperature on biology and life table parameters of the Asian citrus psyllid, Diaphorina citri Kuwayama (Homoptera: Psyllidae). *Ann Appl Biol* 137(3):201–206.
18. Boina DR, Rogers ME, Wang N, Stelinski LL (2010) Effect of pyriproxyfen, a juvenile hormone mimic, on egg hatch, nymph development, adult emergence and reproduction of the Asian citrus psyllid, *Diaphorina citri* Kuwayama. *Pest Manag Sci* 66(4):349–357.
19. Michaud JP (2004) Natural mortality of Asian citrus psyllid (Homoptera: Psyllidae) in central Florida. *Biol Control* 29(2):260–269.
20. Pande YD (1971) Biology of citrus psylla, Diaphorina citri Kuw. (Hemiptera: Psyllidae). *Isr J Entomol* 6(2):307–311.
21. Xu CF, Xia YH, Li KB, Ke C (1988) Further study of the transmission of citrus huanglungbin by a psyllid, Diaphorina citri Kuwayama. *Proceedings of the 10th Conference of the International Organisation on Citrus Virology*, eds Timmer LW, Garnsey SM, Navarro L (University of California, Riverside, CA), pp 243–248.
22. Pelz-Stelinski KS, Brlansky RH, Ebert TA, Rogers ME (2010) Transmission parameters for Candidatus liberibacter asiaticus by Asian citrus psyllid (Hemiptera: Psyllidae). *J Econ Entomol* 103(5):1531–1541.
23. Hall DG, Hentz MG (2011) Seasonal flight activity by the Asian citrus psyllid in east central Florida. *Entomol Exp Appl* 139(1):75–85.
24. Boina DR, Meyer WL, Onagbola EO, Stelinski LL (2009) Quantifying dispersal of Diaphorina citri (Hemiptera: Psyllidae) by immunomarking and potential impact of unmanaged groves on commercial citrus management. *Environ Entomol* 38(4):1250–1258.
25. Ahmad R (1961) Citrus psylla: Its damage, population and efficacy of some insecticides against it. *Pak J Sci* 13(4):195–200.
26. Hall DG, Richardson ML, Ammar E-D, Halbert S (2012) Asian citrus psyllid, Diaphorina citri, vector of citrus huanglongbing. *Entomologia et Applicata* 146(2):207–223.
27. Melbourne BA, Hastings A (2009) Highly variable spread rates in replicated biological invasions: Fundamental limits to predictability. *Science* 325(5947):1536–1539.
28. Bassanezi RB, et al. (2013) Efficacy of area-wide inoculum reduction and vector control on temporal progress of huanglongbing in young sweet orange plantings. *Plant Dis* 97(6):789–796.
29. Croxton SD, Stansly PA (2014) Metalized polyethylene mulch to repel Asian citrus psyllid, slow spread of huanglongbing and improve growth of new citrus plantings. *Pest Manag Sci* 70(2):318–323.
30. Parnell S, Gottwald TR, Gilks WR, van den Bosch F (2012) Estimating the incidence of an epidemic when it is first discovered and the design of early detection monitoring. *J Theor Biol* 305:30–36.
31. Li W, Hartung JS, Levy L (2006) Quantitative real-time PCR for detection and identification of Candidatus Liberibacter species associated with citrus huanglongbing. *J Microbiol Methods* 66(1):104–115.